Importance of satisfying thermodynamic consistency in light emitting diode simulations

Patricio Farrell, Julien Moatti, Michael O'donovan, Stefan Schulz, Thomas Koprucki

Importance of satisfying thermodynamic consistency in light emitting diode simulations

Patricio Farrell[1*], Julien Moatti[4], Michael O'Donovan[1,2,3], Stefan Schulz[2,3] and Thomas Koprucki[1]

[2]Tyndall National Institute, Univers ite College Cork, Cork, T12 R5CP, Ireland.
[3]School of Physics, University College Cork, Cork, T12 YN60, Ireland.
[1]Weierstrass Institute for Applied Analysis and Stochastics (WIAS), Mohrenstr. 39, Berlin, 10117, Germany.
[4]Inria, Univ. Lille, CNRS, UMR 8524 - Laboratoire Paul Painlevé, Lille, F-59000, France.

*Corresponding author(s). E-mail(s): patricio.farrell@wias-berlin.de;
Contributing authors: julien.moatti@inria.fr; michael.odonovan@wias-berlin.de; stefan.schulz@tyndall.ie; thomas.koprucki@wias-berlin.de;

Abstract

We show the importance of using a thermodynamically consistent flux discretization when describing drift-diffusion processes within light emitting diode simulations. Using the classical Scharfetter-Gummel scheme with Fermi-Dirac statistics is an example of such an inconsistent scheme. In this case, for an (In,Ga)N multi quantum well device, the Fermi levels show steep gradients on one side of the quantum wells which are not to be expected. This result originates from neglecting diffusion enhancement associated with Fermi-Dirac statistics in the numerical flux approximation. For a thermodynamically consistent scheme, such as the SEDAN scheme, the spikes in the Fermi levels disappear. We will show that thermodynamic inconsistency has far reaching implications on the current-voltage curves and recombination rates.

Keywords: Scharfetter-Gummel scheme, (In,Ga)N devices, numerical simulations, thermodynamic consistency

1 Introduction

In recent years drift-diffusion simulations have offered a numerically attainable method for studying carrier dynamics in a wide variety of devices including light-emitting diodes (LEDs) [1–3], transistors [4, 5] and solar cells [6, 7]. The physical interpretation of the model is quite straightforward: carriers in a device tend to diffuse from regions of high carrier density to low, and have drift motion due to an applied force such as an electric field in the device. On the other hand, the numerical implementation of the model can carry pitfalls which lead to an incorrect description of the device behaviour as we will highlight below in detail.

The purpose of this publication is therefore to show the practical unphysical implications of disobeying thermodynamic consistency. In the stationary case, thermodynamic consistency for discretized drift-diffusion equations can be defined by the demand that the zero bias solution coincides with the thermodynamic equilibrium. In the transient case, it is closely related to the fact that, for boundary conditions compatible with the thermodynamic equilibrium, the solution converges to this equilibrium when time tends to infinity. It is already known that disobeying this property causes non-physical dissipation in the steady state, see [8]. However, the inconsistent discrete approximation of the numerical fluxes has also more direct consequences for the quasi Fermi potentials and is thus important for accurately describing the physics of a device in the frame of drift-diffusion simulations. If one inconsistently numerically approximates the numerical fluxes, the quasi Fermi level will show a completely wrong behavior in for instance quantum well regions, which are at the heart of modern light emitting diodes. This has a knock-on effect for the description of the carrier densities and thus also recombination and current-voltage (IV) curves, which we will illustrate with an (In,Ga)N quantum well structure, a material system of strong interest for energy efficient solid state lighting [9].

For the Boltzmann distribution, the classical Scharfetter-Gummel scheme [10] presents such a thermodynamically consistent scheme. Strictly monotonically increasing non-Boltzmann distribution functions lead to *diffusion enhancement*. Various extensions of the Scharfetter-Gummel scheme have been suggested to account for this effect, see [11–13]. Unfortunately, these schemes are not thermodynamically consistent. In [14, 15] a thermodynamically consistent generalization for Blakemore statistics (which is itself a special case of [16]) is presented in the spirit of [10] by solving local Dirichlet problems. But this generalization requires solving local nonlinear equations during assembly and the iterative solution of the coupled system. It is therefore computationally prohibitively expensive. A computationally more affordable

approach is presented in [17]. On the other hand, in [8] the author presents another extension of the Scharfetter-Gummel scheme using a proper average of the nonlinear diffusion guaranteeing thermodynamic consistency for a specific choice of the distribution function. An alternative interpretation of this approach based on averaging the diffusion enhancement for a very general class of statistical distribution functions was given in [18]. Finally, the SEDAN scheme [19–21] includes the nonlinearity in the drift instead of the diffusion part of the flux and thus also yields a thermodynamically consistent scheme.

The remainder of this paper is organized as follows: In Section 2, we describe the bipolar drift-diffusion model for charge transport in semiconductors. Its finite volume discretization including the flux discretizations is described in Section 3. The formal definition of discrete thermodynamic consistency is also presented in this section. We compare thermodynamically consistent and inconsistent schemes in Section 4 by studying the distribution of densities and quasi Fermi levels within an (In,Ga)N quantum well (QW) system, which is embedded in a *p-i-n* junction. Finally, we conclude in Section 5.

2 Drift-diffusion equations and diffusion enhancement

We briefly introduce a model based on nonlinear partial differential equations which describes bipolar charge transport in a semiconductor. More details can be found in [22]. The dependence of the carrier densities n and p on the chemical potentials for electrons and holes η_n and η_p are described by a statistical distribution function $\mathcal{F}$ as well as conduction and valence band densities of states N_c and N_v via the state equations $n = N_c\mathcal{F}(\eta_n)$ and $p = N_v\mathcal{F}(\eta_p)$. Typical choices for the distribution function are $\mathcal{F}(\eta) = \exp(\eta)$, the so-called Boltzmann approximation, or $\mathcal{F}(\eta) = F_{1/2}(\eta) = \frac{2}{\sqrt{\pi}}\int_0^\infty \frac{E^{1/2}}{e^{E-\eta}+1}\,dE$, namely the Fermi-Dirac integral of order 1/2 describing degenerate semiconductors.

The chemical potentials are related to the quasi-Fermi potentials of electrons and holes φ_n and φ_p via

$$\eta_n = (q(\psi - \varphi_n) - E_c)/(k_BT) \text{ and } \eta_p = (q(\varphi_p - \psi) + E_v)/(k_BT).$$

Here q denotes the elementary charge, ψ the electrostatic potential, k_B the Boltzmann constant, T the temperature and E_c and E_v the conduction and valence band-edge energies. We model a bipolar semiconductor device as a domain $\Omega \subset \mathbb{R}^d$ where the carrier transport in a self-consistent electrical field is described by a system of partial differential equations. In the steady-state case this drift-diffusion system consists of Poisson's equation for ψ and continuity equations for electrons and holes:

$$-\nabla\cdot(\varepsilon_0\varepsilon_r\nabla\psi) = q(C + p - n), \quad \vec{x}\in\Omega, \tag{1}$$

$$-\nabla\cdot\mathbf{j}_n = -qR, \qquad \nabla\cdot\mathbf{j}_p = -qR, \quad \vec{x}\in\Omega. \tag{2}$$

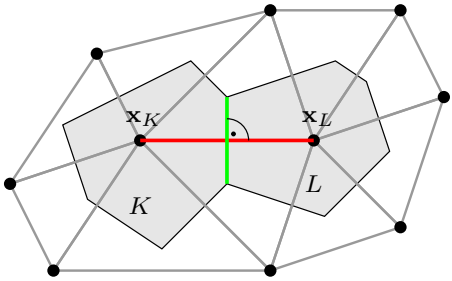

Fig. 1 Collocation points (black), simplices (grey lines) and control volumes (filled) in two space dimensions. Note the right angle between the lines $\overline{\vec{x}_K\vec{x}_L}$ and $\partial K \cap \partial L$, which allows to approximate the normal current through the face boundary $\partial K \cap \partial L$ (green) by a finite difference expression along the edge $\overline{\vec{x}_K\vec{x}_L}$ (red).

Here, ε_r is the relative permittivity, C is the net doping profile, and $R = R(n,p)$ describes the recombination. Electron and hole currents can be expressed in terms of quasi-Fermi potentials by

$$\mathbf{j}_n = -q\mu_n n \nabla\varphi_n, \quad \mathbf{j}_p = -q\mu_p p \nabla\varphi_p, \tag{3}$$

or for any strictly monotonic Fermi-like distribution function $\mathcal{F}(\eta)$ in drift-diffusion form

$$\mathbf{j}_n = q\mu_n \Big[U_T g\Big(\frac{n}{N_c}\Big)\nabla n - n\nabla\left(\psi - \frac{E_c}{q}\right)\Big],$$
$$\text{and } \mathbf{j}_p = -q\mu_p \Big[U_T g\Big(\frac{p}{N_v}\Big)\nabla p + p\nabla\left(\psi + \frac{E_v}{q}\right)\Big], \tag{4}$$

where μ_n and μ_p denote the electron and hole mobilities, respectively, and $U_T = k_B T/q$ is the thermal voltage. The factor g can be defined in terms of densities, $g(x) = x(\mathcal{F}^{-1})'(x)$, for $x \in \mathbb{R}$. This factor is the so-called *diffusion enhancement* appearing as a density-dependent modification factor in the generalized Einstein relation, see [23], leading in general to a non-linear diffusion coefficient. For the Boltzmann distribution, $\mathcal{F}(\eta) = \exp(\eta)$, we have $g \equiv 1$ and the current expressions (4) reduce to the usual ones with linear diffusion.

3 Finite volume space discretization

We discretize the domain Ω using the Voronoï box based finite volume method introduced in [24], also known as "box method" due to [25]. It uses a simplical boundary conforming Delaunay grid ([26]) which allows to obtain control volumes surrounding each given collocation point $\vec{x}_K$ by joining the circumcenters of the simplices containing it, see Fig. 1.

Let ∂K denote the boundary of the control volume K, and $|\xi|$ the measure of a geometrical object ξ. For each control volume K, we integrate the continuity equation (2) and apply Gauss's theorem to the integral of the flux

divergence. Restricting our considerations to the electron transport equation, we obtain

$$\begin{aligned} 0 = \int_{\partial K} \mathbf{j}_n \cdot \vec{n} ds - \int_K qR \, d\vec{x} = \sum_{L \text{ neighbor of } K} \int_{\partial K \cap \partial L} \mathbf{j}_n \cdot \vec{n}_{KL} ds - \int_K qR \, d\vec{x} \\ \approx \sum_{L \text{ neighbor of } K} |\partial K \cap \partial L| j_{n,KL} - q|K|R(n_K, p_K), \end{aligned} \tag{5}$$

where $\vec{n}$ is the internal unit normal to ∂K and $\vec{n}_{KL}$ is the internal unit normal to the interface $\partial K \cap \partial L$ for each neighbor L of K. The values n_K, p_K are the numerical approximations of the densities n and p at the collocation points $\vec{x}_K$, and $j_{n,KL}$ are approximations of the normal currents through $\partial K \cap \partial L$, see Fig. 1. In the same manner the discretization of the Poisson equation can be obtained. A more detailed discussion of this method can be found in [22].

3.1 Discrete thermodynamic consistency

One property which holds on a continuous level to avoid unphysical state dissipation is the *preservation of thermodynamic equilibrium* [22]. Mathematically, this means that vanishing fluxes shall imply constant quasi Fermi potentials. The classical discrete counterpart of this property is formulated as below (see for example [18, 22]): a numerical flux $j = j_{KL}$ is said to be thermodynamically consistent if it satisfies an analogous discrete relation, i.e.

$$j = 0 \quad \text{implies} \quad \delta\varphi_{KL} = 0, \tag{6}$$

where $\delta\varphi_{KL} = (\varphi_L - \varphi_K)/U_T$. Similarly, we define $\delta\eta_{KL} = \eta_L - \eta_K$ and $\delta\psi_{KL} = (\psi_L - \psi_K)/U_T$ and $\delta E_{KL} = (E_{c,L} - E_{c,K})/(qU_T)$. We point out that the condition (6) holds in equilibrium. Here, we introduce a stronger notion of thermodynamic consistency, which holds outside of equilibrium, namely

$$j \leq 0 \text{ implies } \delta\varphi_{KL} \geq 0 \qquad \text{and} \qquad j \geq 0 \text{ implies } \delta\varphi_{KL} \leq 0. \tag{7}$$

An important property of defining thermodynamical consistency like above is that the sign of the numerical current is consistent with that of its continuous counterpart (3). Thermodynamic consistency is also important, when coupling the van Roosbroeck system to heat transport models [22]. We discuss now different numerical fluxes that may be used within a Voronoï finite volume framework.

3.2 The Scharfetter-Gummel scheme

First, we introduce the well known, classical Scharfetter-Gummel flux approximation [10] given by

$$j_{\text{sg}} = j_0 \left\{ B\left(\delta\psi_{KL} - \delta E_{KL}\right) \mathcal{F}(\eta_L) - B\left(-\delta\psi_{KL} + \delta E_{KL}\right) \mathcal{F}(\eta_K) \right\}, \tag{8}$$

where the constant j_0 is given by $j_0 = q\mu_n N_c \dfrac{U_T}{h_{KL}}$ for $h_{KL} = |\vec{x}_K - \vec{x}_L|$, and B is the Bernoulli function, $B(x) = \frac{x}{\exp(x)-1}$. It is important to point out that Scharfetter and Gummel introduced this numerical flux only in the Boltzmann regime, i.e. $\mathcal{F} = \exp$. In this case, the flux is thermodynamically consistent in the sense of (6). However, once we leave the Boltzmann regime, i.e. $\mathcal{F} \neq \exp$, and continue using (8) this numerical flux will no longer be thermodynamically consistent.

3.3 SEDAN scheme

Next, we present the SEDAN scheme, which yields a thermodynamically consistent approach also for state equations which do not necessarily rely on the Boltzmann approximation. The earliest reference we could find for such a excess chemical potential scheme is the source code of the SEDAN III simulator [21], which explains the reason we use this name. A numerical analysis focused comparison of this flux approximation is given in [20] and simulation results are presented in [19]. The scheme is motivated by rearranging the drift part to include the *excess chemical potential*, $\nu^{ex} = \ln \mathcal{F}(\eta) - \eta$, yielding

$$j_{\text{sedan}} = j_0 \left\{ B\left(Q_{KL}\right) \mathcal{F}(\eta_L) - B\left(-Q_{KL}\right) \mathcal{F}(\eta_K) \right\} \tag{9}$$

with

$$Q_{KL} = \delta\psi_{KL} - \delta E_{KL} + \nu_L^{ex} - \nu_K^{ex} = \delta\psi_{KL} - \delta E_{KL} - \delta\eta_{KL} + \ln \frac{\mathcal{F}(\eta_L)}{\mathcal{F}(\eta_K)}. \tag{10}$$

Note that, using the definition of Q_{KL} and the fact that $e^x B(x) = B(-x)$, one can reformulate the SEDAN flux as

$$j_{\text{sedan}} = j_0 B\left(Q_{KL}\right) \mathcal{F}(\eta_L) \left(1 - e^{\delta\varphi_{KL}}\right).$$

Therefore, it is easy to see that the SEDAN flux satisfies (7), since both $B(Q_{KL})$ and $\mathcal{F}(\eta_L)$ are positive: it is a thermodynamicaly consistent numerical flux.

Note that when applying Boltzmann statistics $\nu^{ex} = 0$ and the SEDAN flux becomes equivalent to the Scharfetter-Gummel expression. Therefore, in the next section, when displaying results using Boltzmann statistics, we only show results from one numerical scheme.

4 Simulations

To illustrate the importance of using thermodynamically consistent flux approximations, we study a simple (In,Ga)N multi QW (MQW) system. In particular, we consider three QWs and the same set of parameters as in [3]. For large negative values of η ($\eta \leq -2$, which correspond roughly to densities below 14% of the effective density of states N_c, thus a low carrier density

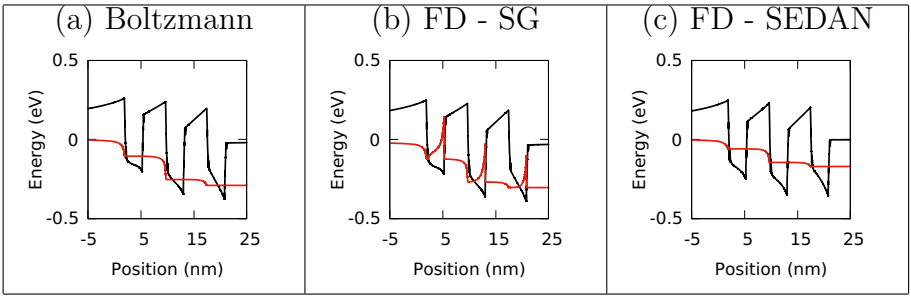

Fig. 2 Conduction band edge (black) and quasi Fermi energy (red) at a bias of 3.3V (a) when using Boltzmann statistics, (b) when incorrectly using the Scharfetter-Gummel (SG) scheme with Fermi-Dirac (FD) statistics, and (c) when correctly using the SEDAN scheme with Fermi-Dirac statistics.

regime in the conduction band of the wells) the Boltzmann approximation provides a good estimate of the Fermi-Dirac statistics. Therefore in certain cases Scharfetter-Gummel scheme can offer a good description of the drift-diffusion model (e.g. Ref. [27]).

On the other hand there are situations where Boltzmann statistics will not suffice. At a bias of 3.3V the importance of using a thermodynamically consistent scheme becomes apparent. The conduction band edge and quasi Fermi energies of the system when treated using Boltzmann statistics is shown in Fig. 2 (a). Applying the Scharfetter-Gummel scheme (8) to Fermi-Dirac statistics for a bias of 3.3V leads to spikes in the Fermi energy on the right side of each QW, see Figure 2 (b).

Recalling the condition (7), for thermodinamically consistent schemes, the discrete gradient of the discrete quasi Fermi level should indicates the direction of the discrete electron flow (as it is in the continuous case, according to (3)). However on figure 2 (b), one can see that, when the Scharfetter-Gummel scheme is applied to Fermi-Dirac statistics, resulting in a thermodynamically *inconsistent* scheme, the direction of electron flow is to the right outside the QW regions (e.g. between 6 nm and 9 nm) but to the left inside the QW regions (e.g. between 2 nm and 5 nm), which is not in accordance with (7). Moreover, as there is no generation of carriers in the system this change in direction of the electron flux is highly unphysical.

These spikes in the quasi Fermi level are not present if one uses the Scharfetter-Gummel scheme with the Boltzmann approximation, which is a thermodynamically *consistent* scheme (Figure 2 (a)). Similarly, using Fermi-Dirac statistics with the SEDAN scheme does not exhibit the unphysical spikes in the Fermi level (Figure 2 (c)).

Another perspective to interpret thermodynamic inconsistency is to note the incorrect interplay between quasi Fermi energies and local current fluxes. We see in Fig. 3 that the local numerical electron fluxes are positive and decrease monotonically across the QW regions. This is true for all three settings, that is, Boltzmann statistics in combination with the classical Scharfetter-Gummel scheme, as well as Fermi-Dirac statistics using both

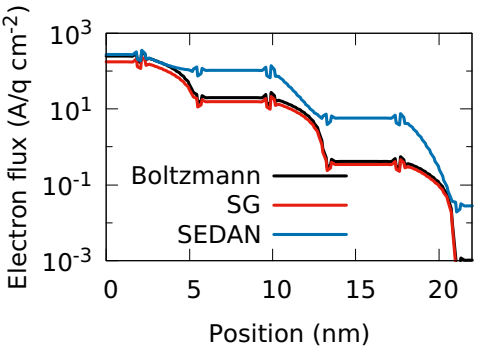

Fig. 3 Numerical electron flux averaged over each atomic plane at a bias of 3.3V shown for Boltzmann statisitcs (black), Fermi-Dirac statistics incorrectly using the Scharfetter-Gummel (SG) flux discretization (red) and Fermi-Dirac statistics correctly using the SEDAN flux discretization (blue).

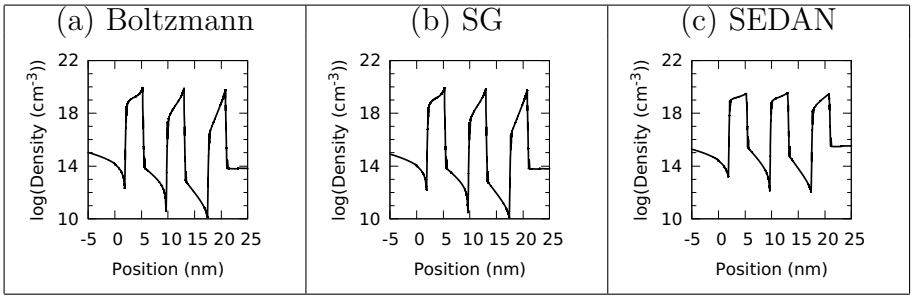

Fig. 4 Electron density at a bias of 3.3V (a) when using Boltzmann statistics, (b) when incorrectly using the Scharfetter-Gummel (SG) scheme with Fermi-Dirac statistics, and (c) when correctly using the SEDAN scheme with Fermi-Dirac statistics.

consistent and inconsistent numerical schemes. By our definition of a thermodynamically consistent scheme (7), a positive local numerical flux should imply a negative quasi Fermi potential discrete gradient. In fact, this is true for both consistent settings as one can see in Fig. 2 (a) and (c). However, for the inconsistent case the derivative of the quasi Fermi energies become positive near the right side of the wells, Fig. 2 (b), also in disagreement of how the flux should behave at the continuous level (see the relation between the flux and the quasi Fermi potential (3)).

Previous studies of the numerical flux approximations have shown that an thermodynamically inconsistent scheme can result in the incorrect sign of the particle flux [18]. This is also reflected by the fact that (6) holds only for consistent schemes, which guarantee the physically correct sign of the current also far from equilibrium.

The physical reason of why an inconsistent scheme produces spikes on the right sides of the QWs becomes apparent when looking at the corresponding densities at a bias of 3.3V. The Fermi-Dirac function grows like a

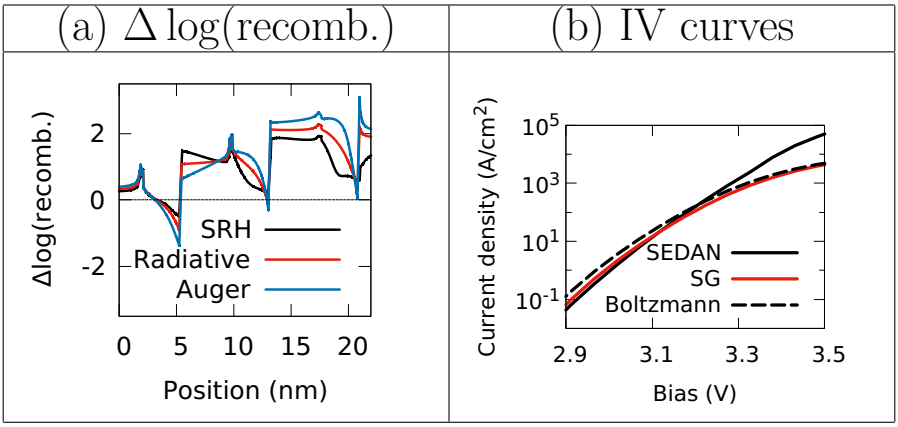

Fig. 5 (a) Difference in magnitude of the Shockley-Read-Hall (SRH, black), radiative (red) and Auger (blue) recombination rates between Fermi-Dirac and Boltzmann statistics at a bias of 3.3V, calculated as described in the main text. (b) Current density-voltage (IV) curves using Boltzmann statistics (black, dashed), Fermi-Dirac statistics using the Scharfetter-Gummel scheme (SG, red) and Fermi-Dirac statistics using the SEDAN scheme (black, solid), shown on a log scale.

polynomial while the Boltzmann approximation grows for large densities exponentially, see for example Figure 50.9 in [22]. This different behaviour leads to nonlinear diffusion, the so-called diffusion enhancement, for non-Boltzmann statistics, see (4), or [18]. The Scharfetter-Gummel scheme neglects the diffusion enhancement assuming only linear diffusion, which has a knock-on impact on the carrier density: the densities calculated using Boltzmann statistics (Fig. 4 (a)) and using Fermi-Dirac statistics with the Scharfetter-Gummel scheme (Fig. 4 (b)) are visibly indistinguishable. However, in order to produce the same density between a Boltzmann and Fermi-Dirac calculation, the quasi Fermi levels must differ. This results in the unusual behaviour of the quasi Fermi level exhibited in Figure 2 (b). Comparing these densities with the correctly calculated density using Fermi-Dirac statistics in combination with the thermodynamically consistent SEDAN scheme (Figure 4 (c)) we see that the choice of statistics function will impact carrier density in both the well and the barrier regions at the here chosen example bias of 3.3V.

Because it influences the carrier density, thermodynamic inconsistency has direct implications for the computed recombination rates as well as the current-voltage (IV) curves. Next, we compare the recombination rates calculated using Boltzmann statistics with those calculated while incorrectly using the Scharfetter-Gummel scheme implementing Fermi-Dirac statistics.

This is highlighted in Figure 5 (a), where the differences between Fermi-Dirac and Boltzmann-like behaviour are shown for the three recombination rates, calculated via

$$\Delta \log(\text{recomb.}) = \log(\mathrm{R}_i^{\mathrm{SEDAN}}) - \log(\mathrm{R}_i^{\mathrm{Boltzmann}}) \ ,$$

where R_i^s is the recombination rate associated with the process i ($i \in$ {Shockley–Read–Hall, Radiative, Auger}) calculated with the scheme s ($s \in$ {Boltzmann, SEDAN}). From this figure it becomes clear that the Boltzmann behaviour overall underestimates the recombination. In particular, near the right-most QW the recombination rates differ by approximately two orders of magnitude. These differences increase as the bias is increased (not shown). This can have consequences for overall device behaviour such as the internal quantum efficiency and the I-V curves. The latter are shown in Figure 5 (b), where the decreased recombination current displayed in the Boltzmann and thermodynamically inconsistent Fermi-Dirac scheme leads to an underestimate of the current density by an order of magnitude at 3.5V.

The results highlighted above indicate that Fermi statistics implemented using a thermodynamically inconsistent scheme will result in Boltzmann-like behaviour in LED simulations – at least in terms of carrier and current densities. If this is extended to *laser* simulations the consequences can be even more dramatic, as the gain calculation depends on the difference between the electron and hole quasi Fermi energies [28], expressed by the so-called Fermi voltage. In this case the unphysical spikes seen in Fig. 2 (b) will lead to an incorrect prediction of the transparency density.

5 Conclusion

In this paper, we have shown the importance of using a thermodynamically consistent flux discretization when describing drift-diffusion processes within quantum well devices.

Using the classical Scharfetter-Gummel scheme with Fermi-Dirac statistics is an example of such an inconsistent scheme. Here we studied an (In,Ga)N multi quantum well structure as an example since it is a very important material system for optoelectronic devices. In this case, the Fermi levels show steep gradients on one side of the quantum wells resulting in an unphysical description of the direction of the current, e.g. assuming the usual continuous expression. This is explained by the omission of diffusion enhancement from the numerical current expression, that leads to a similar density distribution as using Boltzmann statistics. This has a knock-on effect for recombination and current-voltage behaviour, where using Fermi-Dirac statistics with a thermodynamically inconsistent scheme may incorrectly predict a Boltzmann-like behaviour.

Contrarily, for a thermodynamically consistent scheme, such as the SEDAN scheme, these unphysical spikes in the Fermi levels disappear and accurate current curves and recombination processes are predicted. Thus, thermodynamically consistent schemes are essential to address open questions, such as the efficiency drop in modern light emitting devices and to reliably guide their design.

References

[1] Römer F, Witzigmann B (2018) Signature of the ideality factor in III-nitride multi quantum well light emitting diodes. Opt Quant Electron 50(11):1-10

[2] Li CK, Piccardo M, Lu LS, Mayboroda S, Marinelli L, Peretti J, Speck J, Weisbuch C, Filoche M, Wu YR (2017) Localization landscape theory of disorder in semiconductors. III. Application to carrier transport and recombination in light emitting diodes. Phys Rev B 95(04):144206

[3] O'Donovan M, Farrell P, Moatti J, Streckenbach T, Koprucki T, Schulz S (2022) Impact of random alloy fluctuations on the carrier distribution in multi-color (In,Ga)N/GaN quantum well systems. arXiv:2209.11657

[4] Szymańnski MZ, Tu D, Forchheimer R, 2-D Drift-Diffusion Simulation of Organic Electrochemical Transistors. IEEE Transactions on Electron Devices 64(12):5114-5120

[5] Darwish M, Gagliardi A (2020) A drift-diffusion simulation model for organic field effect transistors: on the importance of the Gaussian density of states and traps. J. Phys. D: Appl. Phys. (53):105102

[6] Ren X, Wang Z, Sha WEI, Choy WCH (2017) Exploring the Way To Approach the Efficiency Limit of Perovskite Solar Cells by Drift-Diffusion Model. ACS Photonics 4(4):934-942

[7] Tress W, Leo K, Riede M (2012) Optimum mobility, contact properties, and open-circuit voltage of organic solar cells: A drift-diffusion simulation study. Phys Rev B (85)155201

[8] Bessemoulin-Chatard M (2012) A finite volume scheme for convection-diffusion equations with nonlinear diffusion derived from the Scharfetter-Gummel scheme. Numer Math 121:637–670

[9] Humphreys, CJ (2008) Solid-State Lighting. MRS Bulletin 33(4):459–470

[10] Scharfetter DL, Gummel HK (1969) Large signal analysis of a silicon Read diode. IEEE Trans Electron Dev 16:64–77

[11] Jüngel A (1995) Numerical approximation of a drift-diffusion model for semiconductors with nonlinear diffusion. ZAMM 75(10):783–799

[12] Purbo OW, Cassidy DT, Chisholm SH (1989) Numerical model for degenerate and heterostructure semiconductor devices. J Appl Phys 66(10):5078–5082

[13] Stodtmann S, Lee RM, Weiler CKF, Badinski A (2012) Numerical simulation of organic semiconductor devices with high carrier densities. J Appl Phys 112(11):114,909

[14] Koprucki T, Gärtner K (2013) Discretization scheme for drift-diffusion equations with strong diffusion enhancement. Opt Quant Electron 45(7):791–796

[15] Koprucki T, Gärtner K (2013) Generalization of the Scharfetter-Gummel scheme. In: Numerical Simulation of Optoelectronic Devices (NUSOD), 2013 13th International Conference on, pp 85–86

[16] Eymard R, Fuhrmann J, Gärtner K (2006) A finite volume scheme for nonlinear parabolic equations derived from one-dimensional local dirichlet problems. Numer Math 102:463–

[17] Chainais-Hillairet C, Eymard R, Fuhrmann J (2022) A monotone numerical flux for quasilinear convection diffusion equation https://hal.archives-ouvertes.fr/hal-03791166/file/art_cef.pdf

[18] Koprucki T, Rotundo N, Farrell P, Doan DH, Fuhrmann J (2015) On Thermodynamic Consistency of a Scharfetter-Gummel Scheme Based on a Modified Thermal Voltage for Drift-Diffusion Equations with Diffusion Enhancement. Opt Quant Electron 47(6):1327-–1332

[19] Abdel D, Farrell P, Fuhrmann J (2021) Assessing the quality of the excess chemical potential flux scheme for degenerate semiconductor device simulation. Opt Quant Electron 53(163)

[20] Cancès C, Chainais-Hillairet C, Fuhrmann J, Gaudeul B (2020) A numerical-analysis-focused comparison of several finite volume schemes for a unipolar degenerate drift-diffusion model. IMA Journal of Numerical Analysis DOI: 10.1093/imanum/draa002

[21] Yu Z, Dutton R (1988) SEDAN III – A one-dimensional device simulator. www-tcad.stanford.edu/tcad/programs/sedan3.html

[22] Farrell P, Doan DH, Kantner M, Fuhrmann J, Koprucki T, Rotundo N (2017) Drift-diffusion models. In: Optoelectronic Device Modeling and Simulation: Fundamentals, Materials, Nanostructures, LEDs, and Amplifiers, CRC Press Taylor & Francis Group, pp 733–771

[23] van Mensfoort SLM, Coehoorn R (2008) Effect of Gaussian disorder on the voltage dependence of the current density in sandwich-type devices based on organic semiconductors. Phys Rev B 78(8):085,207

[24] Macneal RH (1953) An asymmetrical finite difference network. Quart Math Appl 11:295–310

[25] Bank RE, Rose DJ (1987) Some error estimates for the box method. SIAM J Numer Anal 24(4):777–787

[26] Si H, Gärtner K, Fuhrmann J (2010) Boundary conforming Delaunay mesh generation. Comput Math Math Phys 50:38–53

[27] O'Donovan M, Farrell P, Streckenbach T, Koprucki T, Schulz S (2022) Multiscale simulations of uni-polar hole transport in (In,Ga)N quantum well systems. Opt Quant Electron 54(405)

[28] Bandelow U, Gajewski H, Hünlich R (2005) Fabry-Perot Lasers: Thermodynamics-Based Modeling. In: Optoelectronic Devices: Advanced Simulation and Analysis, Springer New York, pp 63–85